Volume 53 | Number 50 | 25 June 2017 | Pages 6663–6802

ChemComm

Chemical Communications

rsc.li/chemcomm

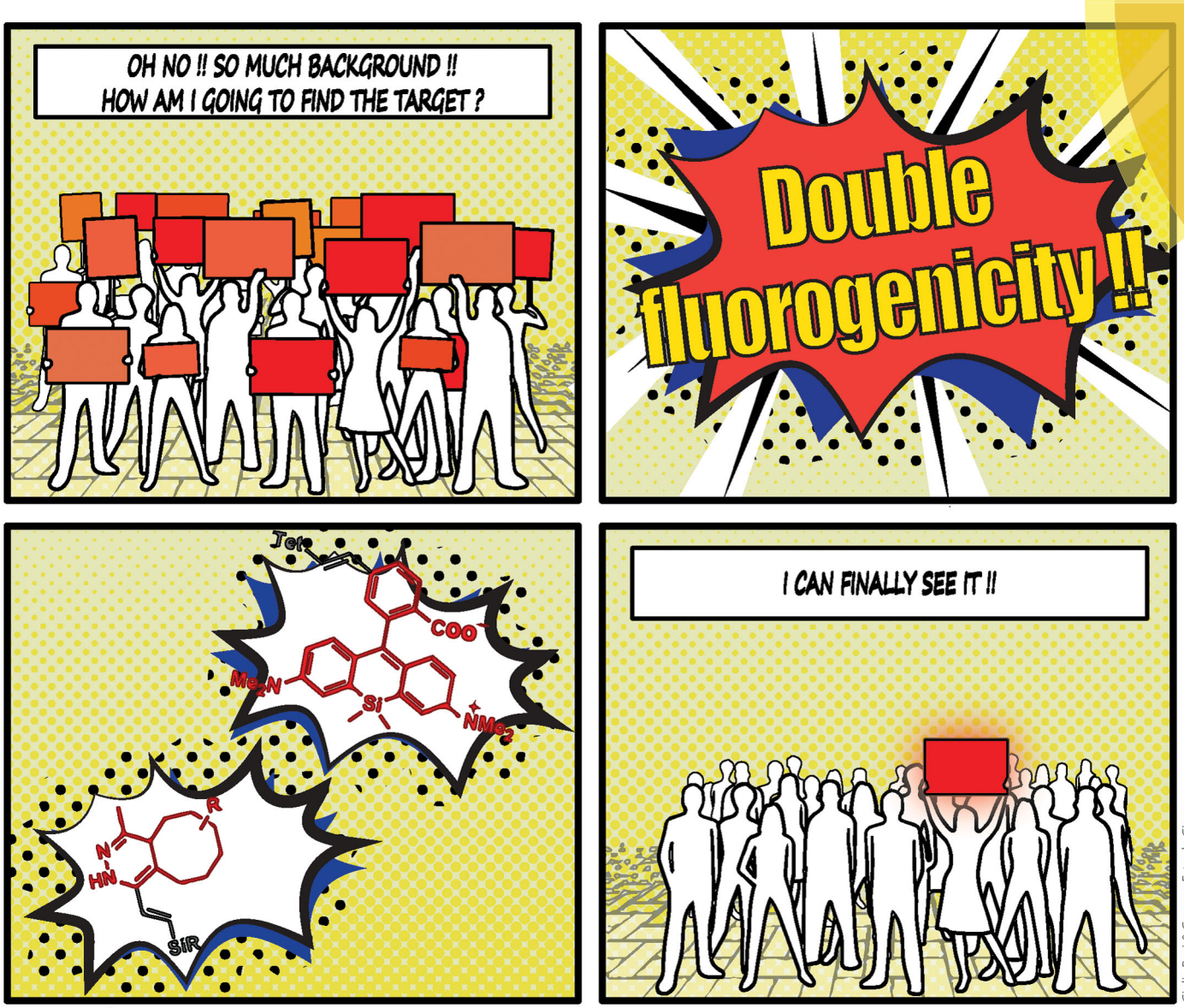

Giulia Paci & Gemma Estrada Girona

ISSN 1359-7345

ROYAL SOCIETY OF CHEMISTRY

COMMUNICATION

P. Kele *et al.*

Bioorthogonal double-fluorogenic siliconrhodamine probes for intracellular super-resolution microscopy

ChemComm

COMMUNICATION

View Article Online
View Journal | View Issue

Cite this: *Chem. Commun.*, 2017, 53, 6696

Received 23rd March 2017,
Accepted 11th May 2017

DOI: 10.1039/c7cc02212c

rsc.li/chemcomm

Bioorthogonal double-fluorogenic siliconrhodamine probes for intracellular super-resolution microscopy†

E. Kozma,[a] G. Estrada Girona,[b] G. Paci,[b] E. A. Lemke[b] and P. Kele*[a]

A series of double-fluorogenic siliconrhodamine probes were synthesized. These tetrazine-functionalized, membrane-permeable labels allowed site-specific bioorthogonal tagging of genetically manipulated intracellular proteins and subsequent imaging using super-resolution microscopy.

Recent years have brought substantial progress in the field of super-resolution microscopy (SRM) enabling the exploration of biomolecular processes in the sub-diffraction range.[1] Although the emerged SRM techniques have revealed fine details of live organisms, there is still room for further improvements. Nowadays, the unavailability of dyes suitable for site-specific tagging of intracellular biomolecules is considered as the biggest limitation of SRM techniques.[2] Ideal small-sized organic fluorophores can be synthetically tailored in order to meet the criteria necessary for intracellular SRM imaging of live cells. Such criteria are as follows: (a) both the labels themselves and the chemistry applied for tagging should be biocompatible, (b) their photophysical characteristics should allow minimal background and autofluorescence in order to result in a high signal-to-noise (S/N) ratio, (c) their fluorescence should be bright and not or minimally impaired by photobleaching and (d) they should be able to transit through membranes. As for the chemistry applied for installation of such probes, bioorthogonal reactions are extremely useful as they are fully biocompatible.[3] Among these transformations, inverse electron demand Diels–Alder (IEDDA) reactions between tetrazines and strained unsaturated ring systems enable the fastest reactions.[4] In order to minimize phototoxicity and autofluorescence, far-red/near-infrared (NIR) emitting fluorophores (650–900 nm) are especially well suited, while background fluorescence of unreacted probes bound non-specifically to hydrophobic surfaces can be reduced efficiently by the use of fluorogenic species.[5,6]

Our continuing efforts to develop fluorescent probes that combine the above listed features have resulted in several bioorthogonally applicable fluorogenic probes with various excitation/emission characteristics.[7] Lately, our attention turned to tetrazine quenched fluorescent frameworks as tetrazines can act both as bioorthogonal handles and quencher moieties.[7d] Tetrazines can exert their quenching effect either by Förster-resonance energy transfer (FRET) or through-bond energy transfer (TBET) mechanisms.[8,9] FRET-based fluorogenic probes are limited to tetrazine–fluorophore pairs where the absorption band of the tetrazine (typically between 520 and 540 nm) overlaps with the emission band of the fluorophore. TBET-based systems, on the other hand, are not constrained by the emission band of the fluorescent unit and, in theory, any kind of fluorophore–tetrazine pairs are suitable upon proper design. Moreover, TBET-based quenching is much faster and more efficient, thus enhancement of the fluorescence signal can reach up to 11 000-fold upon the IEDDA reaction with dienophiles.[9a] The tetrazine-based TBET-quenching approach has already been applied to various fluorophores, yet, it has not been performed on SRM compatible dyes.[9] However, techniques like SRM would greatly benefit from the high signal-to-noise ratio offered by the TBET-mechanism.

Siliconrhodamine (SiR) is a widely used membrane-permeable NIR dye for SRM applications.[10] Besides the high photostability and brightness, the unique environment-dependent fluorescence of carboxy-SiRs due to a polarity dependent lactone-formation offers an appealing opportunity to distinguish between specific and non-specific labeling (polarity-based fluorogenicity).[10] When bound to polar protein surfaces, carboxyl-SiRs exist in a fluorescent zwitterionic form, while upon non-specific adhesion to hydrophobic surfaces, they close to a non-fluorescent spirolactone (Fig. 1). SiR derivatives were applied in voltage sensing, *in vivo* tumor imaging, photodynamic therapy and multicolour imaging studies as well.[11] Despite their wide applications, there are only a few examples of SiR-based probes for site-specific labeling of proteins.[10a,12,13]

[a] "Lendület" Chemical Biology Research Group, Institute of Organic Chemistry, Research Centre for Natural Sciences, Hungarian Academy of Sciences, Magyar tudósok krt. 2, 1117 Budapest, Hungary. E-mail: kele.peter@ttk.mta.hu
[b] Structural and Computational Biology Unit, Cell Biology and Biophysics Unit, European Molecular Biology Laboratory, Meyerhofstrasse 1, Heidelberg, D-69117, Germany

† Electronic supplementary information (ESI) available. See DOI: 10.1039/c7cc02212c

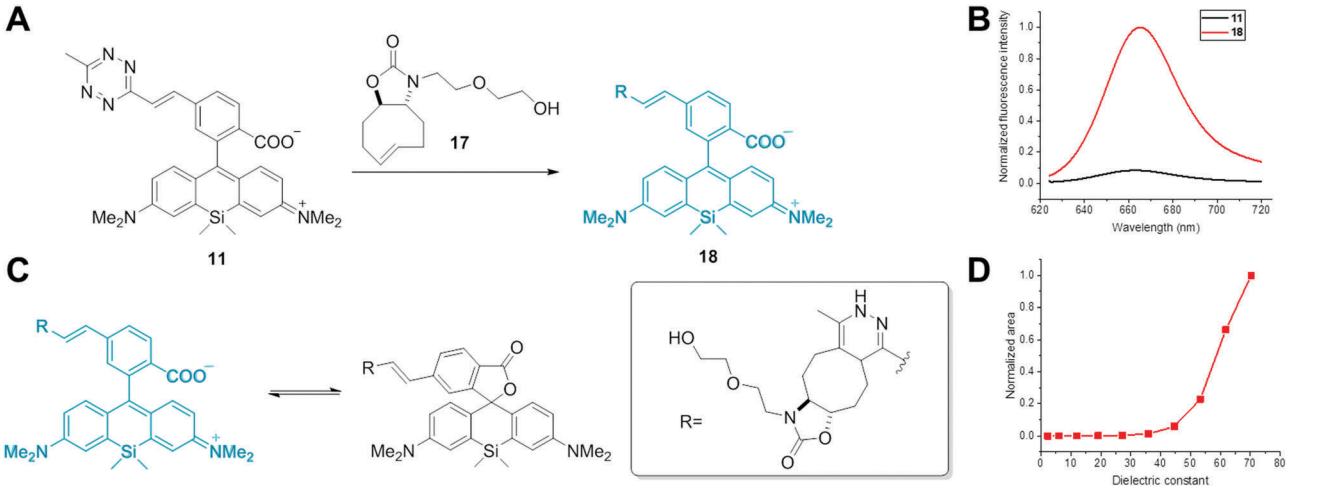

Fig. 1 (A) Fluorogenicity of SiR dyes: the IEDDA reaction between **11** and **17** resulting in fluorescence turn-on upon the formation of conjugate **18** due to the transformation of the quenching tetrazine moiety into dihydropyridazine during the reaction. (B) The corresponding fluorescence emission spectra of free dye **11** (black) and conjugate **18** (red) showing fluorescence turn-on upon the reaction. (C) Polarity-dependent fluorogenicity of SiR dyes: conjugate **18** is present in a fluorescent open, zwitterionic form in a polar environment, and in a non-fluorescent closed spirolactone form in apolar solvents. (D) Normalized integral of fluorescence spectra of **18** in water–dioxane mixtures as a function of dielectric constant. Conjugate **18** is in a fluorescent zwitterionic form in solvents with dielectric constant >50.

Furthermore, no TBET-based carboxyl-SiR fluorogenic probes have been reported yet.

Herein we report the first set of bioorthogonally applicable, NIR-emitting, membrane permeable, double fluorogenic probes suitable for SRM imaging with exceptionally high turn-on rates compared to previously reported tetrazine-based NIR dyes.[9d] We demonstrate the power of the developed SiR-dyes in site-specific labeling of intracellular skeletal proteins and subsequent SRM imaging applications.

TBET-based fluorogenic probes are composed of a donor fluorophore and an acceptor tetrazine unit that are linked together with a conjugated but electronically decoupled (twisted) linker.[14] The tetrazine moiety can be installed onto the phenyl group of SiR directly or *via* alkene, alkyl and phenyl linkers. Former examples showed that incorporation of the tetrazine through direct conjugation or *via* alkyl-linkers into fluorophores is less efficient.[9c,d,f] Therefore we decided to apply alkene and phenyl linkers to connect the tetrazine to carboxy-SiR. Devaraj and co-workers and also our group have recently reported Heck- and Suzuki-type cross-coupling reactions to connect methyl-substituted tetrazines to fluorophores.[7d,9b] To this end we have synthesized Br-substituted intermediate **6**. The general synthetic route for SiR derivatives proceeds through a Si–xantone intermediate which is reacted with aryl lithium reagents *via* nucleophilic addition.[10a] Through this route, however, introduction of halogen-substituted aromatic rings is problematic. Therefore we proceeded *via* an aldehyde condensation reaction developed by Wang *et al.* (Scheme 1) and acquired Br-SiR derivative **6**.[15a]

We positioned the Br-substituent at the 6-position as previous reports showed superior fluorogenic properties of 6-substituted rhodamine derivatives compared to 5-substitution.[9d,f] Pd-Catalyzed cross-coupling reactions of **6** with methyl vinyltetrazine precursor (**8**) and methyltetrazine phenylboronic acid pinacol ester (**10**)

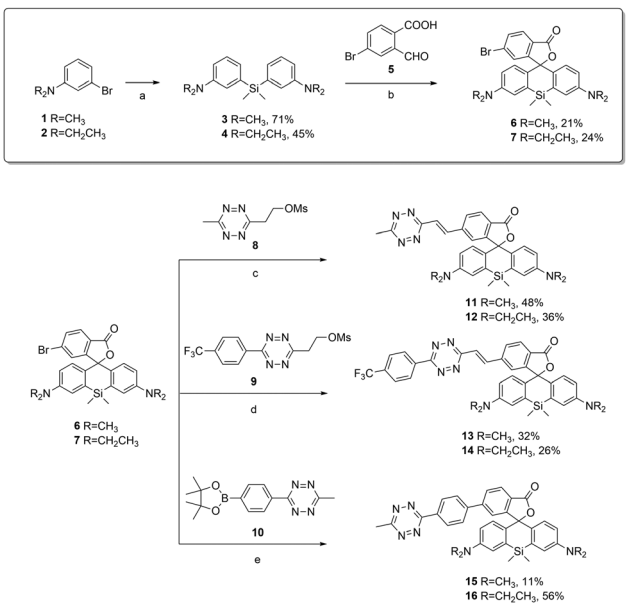

Scheme 1 Synthesis of SiR dyes **11–16**. Reaction conditions: (a, i) *n*-BuLi, THF, −78 °C, 2 h; (ii) $SiCl_2Me_2$, rt, 16 h; (b) $CuBr_2$, 140 °C, 16 h; (c) $Pd_2(dba)_3$, QPhos, $(Cy)_2NMe$, DMF, 50 °C, 40 min, MW; (d) $Pd_2(dba)_3$, QPhos, DIPEA, 1,4-dioxane, 90–110 °C, 16 h; (e) $PdCl_2(dppf)$, Cs_2CO_3, 1,4-dioxane, 90 °C, 16 h.

resulted in alkene-(**11**) and phenyl-linked SiR-tetrazine (**15**), respectively, in moderate to good yields (11–48%). To improve the reaction rate of alkene-linked SiR-tetrazine in IEDDA, we designed a derivative with a trifluoromethyl-phenyl substituent. Electron-withdrawing groups are known to markedly increase the reactivities of tetrazines in IEDDA reactions.[4a] To this end, we synthesized trifluoromethyl-tetrazine (**9**) in two steps *via* $Zn(OTf)_2$ catalyzed Pinner-synthesis and subsequent *O*-mesylation.[15b] Heck reaction of tetrazine **9** with compound **6** proceeded with moderate

yields (32%). It is known that different *N*-alkylation patterns on the rhodamine core can markedly alter the spectral characteristics and brightness of probes.[16] Rotation about the C–N bond in $-NMe_2$ substituted rhodamines leads to faster decay of the excited state and hence to lowered quantum yield. Thus we synthesized $-NEt_2$ substituted derivatives (**12**, **14**, **16**) starting from Br-SiR derivative **7**, which have restricted C–N bond rotation compared to $-NMe_2$ derivatives.

Next, we characterized the spectral properties of SiR-tetrazines **11–16**. Measurements were conducted in water containing 0.01% SDS to prevent aggregation of the dyes.[10a] Excitation maxima were found to be at around 645 nm and 655 nm, and fluorescence emission was detected at around 665 nm and 670 nm for the dimethylamino- and diethylamino-derivatives, respectively (Table 1 and Fig. S1, see the ESI†). We measured the fluorogenic properties of the probes in an IEDDA reaction with OxTCO (**17**) (Fig. 1 and Fig. S2, ESI,† Table 1).[7d] To our delight, all derivatives showed much larger fluorescence enhancements (FE) than previously reported fluorogenic tetrazine NIR dyes (*cf.* 5.6×).[9d] We propose that this is attributed to the double fluorogenic nature of our SiR dyes. Among dimethylamine derivatives, phenyl-linked **15** showed the highest turn-on ratio (31×). As expected, ethyl substitution on the N-atom improved turn-on rates of the dyes, and up to 49-fold increase was observed. Although energy transfer occurs from the excited state, interestingly, the extinction coefficients were measured to be lower than ε of the parent fluorophores (Table 1).

The second order rate constants were also determined and were in good agreement with k_2 values of previously reported methyl-tetrazine derivatives with similarly reactive TCO* (for values see the ESI†).[17] As expected, trifluoromethylphenyl derivatives, **13** and **14** reacted much faster than methyl derivatized congeners with OxTCO (**17**) (Fig. S3, ESI†). Due to the lower electron density of the tetrazines in **13** and **14** IEDDA reactions went to completion within minutes compared to methyl substituted probes where the reaction required *ca.* 1.5 h.

We also investigated the polarity dependent absorbance of the Diels–Alder product of alkene-SiR (**18**). In agreement with previous findings, in solvents with lower dielectric constants, absorption maximum characteristic of the spirolactone form at 290 nm was dominant. In polar solvents, however, the zwitterionic form with a characteristic absorption at 645 nm dominated the spectrum (Fig. S4, ESI†). As a consequence, in solvents with dielectric constants <50 conjugate **18** was non-fluorescent while fluorescence gradually reinstated with increasing polarity (Fig. 1).

With the SiR-dyes in hand, showing exceptional fluorogenicity in the NIR region, we were eager to evaluate their performance in the cellular environment. We sought to utilize the genetic code expansion (GCE) technology for site-specific labeling with the newly developed double-fluorogenic probes. We and others have recently shown that non-canonical amino acids (ncAA) with strained alkene and alkyne moieties can be genetically encoded in mammalian cells using the pyrrolysine $tRNA^{Pyl}$/PylRS pair from the *Methanosarcina* species.[18] We used the previously reported skeletal protein vimentin^{116TAG}-mOrange to test the intracellular labeling ability of the dyes.[13,18e] Using the orthogonal $tRNA^{Pyl}$/$PylRS^{AF}$ pair we genetically encoded commercially available cyclooctynylated-lysine (Lys(ε-*N*-BCN^{endo}), Fig. S5, ESI†) into vimentin^{116TAG}-mOrange and performed live cell labeling experiments with dyes **11–16** in mammalian cells. Clear live cell labeling was observed with dye **11** and **12** (Fig. 2), and even with concentrations as low as 1.5 μM within 10 min at 37 °C (for additional images at different concentrations and labeling times see Fig. S6 and S7 (ESI†), and for a comparison of different post-labeling wash times see Fig. S8, ESI†). The labeling was specific without strong background fluorescence (as quantified by channel colocalisation in Fig. S9, ESI†). Less efficient labeling was observed with phenyl-linked dyes **15** and **16**, which is probably due to their slower kinetics (Fig. S10, ESI†). Although CF_3-dyes **13** and **14** showed the fastest labeling properties *in vitro*, they did not give any specific labeling *in vivo* (results not shown). We attribute this to the low polarity of these dyes, which probably impairs their ability to cross the cell-membrane or to label the protein specifically.

To date, there have only been a few reports on bioorthogonally applicable, fluorogenic tetrazine-mediated intracellular labeling inside living cells and subsequent SRM.[13,18e,19] Among them, to

Table 1 Photophysical properties of SiR dyes **11–16**

Dye	$\lambda_{exc(max)}$[a] [nm]	$\lambda_{em(max)}$[a] [nm]	ε_{max}[a,b] [M^{-1} cm^{-1}]	ϕ_F[a,c]	$\Delta\phi_F$[d]	FE[e]
11	643(645)	665(667)	19 700(19 200)	0.016(0.34)	21	22
12	653(652)	671(672)	20 600(19 800)	0.015(0.80)	50	49
13	647(648)	662(665)	26 200(22 500)	0.028(0.26)	9	6
14	655(654)	673(672)	29 000(25 600)	0.037(0.27)	7	8
15	645(644)	660(660)	23 000(21 600)	0.012(0.34)	28	31
16	651(652)	671(670)	26 000(23 900)	0.015(0.53)	35	40

[a] Values refer to tetrazine-dyes while values in parentheses are that of the respective conjugates with **17**. [b] Measured at absorption maxima of the species. [c] Cresyl violet in MeOH was used as the quantum yield reference (ϕ_F = 0.53). [d] Quantum yield ratios of conjugates with **17** and tetrazine-dyes in 0.1% SDS in water. [e] Fluorescence intensity enhancements upon the reaction with **17** in 0.1% SDS in water at emission maxima of the products.

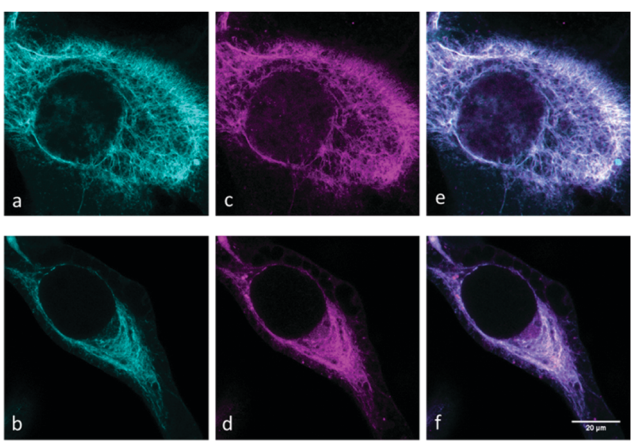

Fig. 2 Confocal images of live cell SiR-labeling of vimentin^{BCNendo}-mOrange with dyes **11** (a, c and e) and **12** (b, d and f). Left to right: mOrange reference channel (a and b), SiR labeling channel (c and d), and overlay (e and f). Labeling was performed at 3 μM for 10 min at 37 °C.

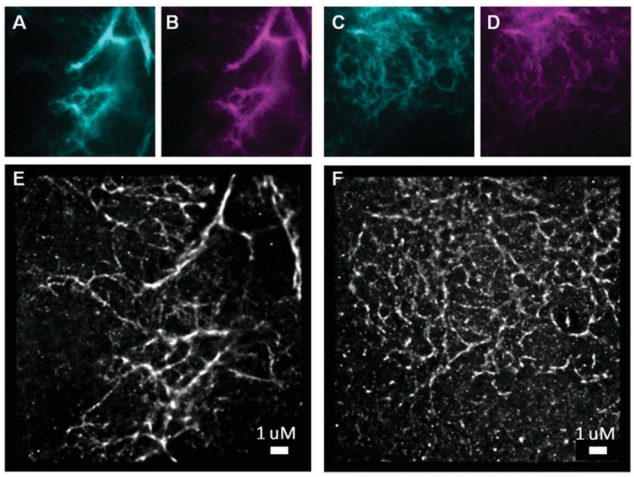

Fig. 3 SRM imaging of vimentin^{BCNendo}-mOrange labeled with dye **11**. Panels (A and C) (cyan) and (B and D) (magenta) show the mOrange and SiR reference channels, respectively for the corresponding SRM images in panels (E and F) from dye **11** labeling (3 μM for 30 minutes at 37 °C). SRM images (E and F) have resolutions of 35 nm and 28 nm respectively as determined by the Fourier ring correlation criterion (FRC).[20]

the best of our knowledge, there have been no reports of site-specific labeling with TBET-based fluorogens. We set out to test the suitability of dyes **11** and **12** in SRM of vimentin. While GSDIM (ground state depletion microscopy followed by individual molecule return)[21] SRM with TIRF illumination was possible with vimentin^{BCNendo}-mOrange labeled with dye **11**, we did not get any specific SRM signal with diethyl-derivative **12** (results not shown). SRM imaging with SiR-**11** (Fig. 3E and F) clearly gives enhanced resolution compared to the reference channels (Fig. 3A–D and Fig. S11, ESI†).

In conclusion, we have developed double-fluorogenic siliconrhodamine-tetrazine probes with improved kinetics and enhanced fluorescence turn-on ratios in the NIR region upon inverse electron demand Diels–Alder reactions. We have demonstrated the effect of the linker and *N*-alkylation pattern of the SiR-tetrazine core on the labeling efficiency using confocal microscopy. We successfully applied one derivative in site-specific super-resolution imaging of a cytoskeletal protein, vimentin. Such probes with distinct spectral characteristics would allow multicolor super-resolution imaging of various intracellular structures.

The present work was supported by the Hungarian Scientific Research Fund (OTKA, NN-116265) and the ''Lendület'' Program of the Hungarian Academy of Sciences (LP2013-55/2013). E. K. is grateful for the support of The New National Excellence Program of The Ministry of Human Capacities (Hungary). EAL acknowledges the SPP1623 and SFB1129 for funding.

Notes and references

1 (*a*) M. Heilemann, *J. Biotechnol.*, 2010, **149**, 243; (*b*) B. Huang, H. Babcock and X. Zhuang, *Cell*, 2010, **143**, 1047.
2 (*a*) M. Fernández-Suárez and A. Y. Ting, *Nat. Rev. Mol. Cell Biol.*, 2008, **9**, 929; (*b*) T. J. Chozinski, L. A. Gagnon and J. C. Vaughan, *FEBS Lett.*, 2014, **588**, 3603.
3 (*a*) C. P. Ramil and Q. Lin, *Chem. Commun.*, 2013, **49**, 11007; (*b*) J. A. Prescher and C. R. Bertozzi, *Nat. Chem. Biol.*, 2005, **1**, 13; (*c*) E. M. Sletten and C. R. Bertozzi, *Angew. Chem., Int. Ed.*, 2009, **48**, 6974.
4 (*a*) A.-C. Knall and C. Slugovc, *Chem. Soc. Rev.*, 2013, **42**, 5131; (*b*) E. Kozma, O. Demeter and P. Kele, *ChemBioChem*, 2017, **18**, 486.
5 (*a*) G. Cserép, A. Herner and P. Kele, *Methods Appl. Fluoresc.*, 2015, **3**, 042001; (*b*) L. D. Lavis and R. T. Raines, *ACS Chem. Biol.*, 2014, **9**, 855.
6 A. Nadler and C. Schultz, *Angew. Chem., Int. Ed.*, 2013, **52**, 2408.
7 (*a*) A. Herner, I. Nikić, M. Kállay, E. A. Lemke and P. Kele, *Org. Biomol. Chem.*, 2013, **11**, 3297; (*b*) A. Herner, G. Estrada Girona, I. Nikić, M. Kállay, E. A. Lemke and P. Kele, *Bioconjugate Chem.*, 2014, **25**, 1370; (*c*) O. Demeter, E. A. Fodor, M. Kállay, G. Mező, K. Németh, P. T. Szabó and P. Kele, *Chem. – Eur. J.*, 2016, **22**, 6382; (*d*) G. Knorr, E. Kozma, A. Herner, E. A. Lemke and P. Kele, *Chem. – Eur. J.*, 2016, **22**, 8972.
8 (*a*) N. K. Devaraj, S. Hilderbrand, R. Upadhyay, R. Mazitschek and R. Weissleder, *Angew. Chem., Int. Ed.*, 2010, **49**, 2869; (*b*) J. Yang, J. Šečkutė, C. M. Cole and N. K. Devaraj, *Angew. Chem., Int. Ed.*, 2012, **51**, 7476.
9 (*a*) L. G. Meimetis, J. C. T. Carlson, R. J. Giedt, R. H. Kohler and R. Weissleder, *Angew. Chem., Int. Ed.*, 2014, **53**, 7531; (*b*) H. Wu, J. Yang, J. Šečkute and N. K. Devaraj, *Angew. Chem., Int. Ed.*, 2014, **53**, 5805; (*c*) A. Wieczorek, T. Buckup and R. Wombacher, *Org. Biomol. Chem.*, 2014, **12**, 4177; (*d*) A. Wieczorek, P. Werther, J. Euchner and R. Wombacher, *Chem. Sci.*, 2017, **8**, 1506; (*e*) P. Agarwal, B. J. Beahm, P. Shieh and C. R. Bertozzi, *Angew. Chem., Int. Ed.*, 2015, **54**, 11504; (*f*) J. C. T. Carlson, *et al.*, *Angew. Chem., Int. Ed.*, 2013, **52**, 6917.
10 (*a*) G. Lukinavičius, *et al.*, *Nat. Chem.*, 2013, **5**, 132; (*b*) S. Uno, *et al.*, *Nat. Chem.*, 2014, **6**, 681; (*c*) P. Shieh, M. S. Siegrist, A. J. Cullen and C. R. Bertozzi, *Proc. Natl. Acad. Sci. U. S. A.*, 2014, **111**, 5456.
11 Y. Kushida, T. Nagano and K. Hanaoka, *Analyst*, 2015, **140**, 685.
12 T. Peng and H. C. Hang, *J. Am. Chem. Soc.*, 2016, **138**, 14423.
13 C. Uttamapinant, *et al.*, *J. Am. Chem. Soc.*, 2015, **137**, 4602.
14 (*a*) T. G. Kim, *et al.*, *J. Phys. Chem. A*, 2006, **110**, 20; (*b*) M. Steeger, S. Griesbeck, A. Schmiedel, M. Holzapfel, I. Krummenacher, H. Braunschweig and C. Lambert, *Phys. Chem. Chem. Phys.*, 2015, **17**, 11848.
15 (*a*) B. Wang, X. Chai, W. Zhu, T. Wang and Q. Wu, *Chem. Commun.*, 2014, **50**, 14374; (*b*) J. Yang, M. R. Karver, W. Li, S. Sahu and N. K. Devaraj, *Angew. Chem., Int. Ed.*, 2012, **51**, 5222.
16 J. B. Grimm, B. P. English, J. Chen, J. P. Slaughter, Z. Zhang, A. Revyakin, R. Patel, J. J. Macklin, D. Normanno, R. H. Singer, T. Lionnet and L. D. Lavis, *Nat. Methods*, 2015, **12**, 244.
17 J. E. Hoffmann, T. Plass, I. Nikić, I. V. Aramburu, C. Koehler, H. Gillandt, E. A. Lemke and C. Schultz, *Chem. – Eur. J.*, 2015, **21**, 12266.
18 (*a*) T. Plass, *et al.*, *Angew. Chem., Int. Ed.*, 2012, **51**, 4166; (*b*) I. Nikić, T. Plass, O. Schraidt, J. Szymański, J. A. Briggs, C. Schultz and E. A. Lemke, *Angew. Chem., Int. Ed.*, 2014, **53**, 2245; (*c*) E. Kozma, I. Nikić, B. R. Varga, I. V. Aramburu, J. H. Kang, O. T. Fackler, E. A. Lemke and P. Kele, *ChemBioChem*, 2016, **17**, 1518; (*d*) K. Lang, L. Davis, J. Torres-Kolbus, C. Chou, A. Deiters and J. W. Chin, *Nat. Chem.*, 2012, **4**, 298; (*e*) I. Nikić, *et al.*, *Angew. Chem., Int. Ed.*, 2016, **55**, 16172.
19 R. S. Erdmann, *et al.*, *Angew. Chem., Int. Ed.*, 2014, **53**, 10242.
20 N. Banterle, *et al.*, *J. Struct. Biol.*, 2013, **183**, 363.
21 J. Fölling, *et al.*, *Nat. Methods*, 2008, **5**, 943.